Graphite oxide nanocoatings as a sustaibale route to extend the applicability of biopolymer-based film

Graphite oxide nanocoatings as a sustaibale route to extend the applicability of biopolymer-based film

Kun Li,[1] Alberto Fina,[2] Daniele Marrè,[3] Federico Carosio,[2] Orietta Monticelli[1*]*

[1]Dipartimento di Chimica e Chimica Industriale, Università di Genova, Via Dodecaneso, 31, 16146 Genova, Italy

[2]Dipartimento di Scienza Applicata e Tecnologia, Politecnico di Torino-sede di Alessandria, viale Teresa Michel, 5, 15121 Alessandria, Italy

[3]Dipartimento di Fisica, Università di Genova, Via Dodecaneso, 33, 16146 Genova, Italy

federico.carosio@polito.it

orietta.monticelli@unige.it

Abstract. In this work, an environmental friendly method was developed and applied for the first time to modify the properties and extend the applicability of polylactic acid (PLA), a biopolymer of great industrial interest. To this aim, the Layer-by-Layer assembly of multilayered coatings comprising graphite oxide (GO) in combination with either chitosan or branched polyethylenimine was employed to modify the surface functional properties of the films, without affecting the bulk. Surface analyses by contact angle measurements and electron microscopy demonstrated the formation of a uniform GO layer, which enhanced the surface hydrophilicity. A 10 bi-layer coated film showed oxygen permeability reduced by 70% in both dry and humid conditions, compared to the neat PLA film. The use of a water soluble reducing agent allowed for the effective room temperature reduction of the GO deposited within the film, as evidenced by IR and contact angle measurements. GO reduction resulted in a significantly decreased surface resistivity and remarkable antistatic properties, suggesting possible applications in the field of antistatic packaging.

Keywords. PLA, surface modification, Layer-by-Layer, graphite oxide, antistatic materials, permeability.

1. Introduction

The challenge for the large-scale exploitation of polymers from renewable resources, as alternative to fossil based polymers, is mainly related to their production costs and properties.[1] On this basis, the methods applied for improving their characteristics or disclosing new properties have to take into account the economic impact while maintaining the "bio" nature of the material [1]. One of the most promising and widely applied biopolymers is polylactic acid (PLA), which is mainly used as packaging material [2,3]. However, in applications requiring high gas barrier, the exploitation of PLA is critical and requires a further reduction of its gas permeability, which may be achieved by different strategies, based mainly on the bulk inclusion of organic or inorganic additives [2,3].

In several packaging applications, antistatic properties are also required, which are traditionally obtained by the bulk inclusion of organic antistatic agents, which form electrostatic discharge channels upon migration onto the surface and by absorbing moisture [4,5]. A relevant drawback of this method is that long-term antistatic effects cannot be maintained due to additive loss from the polymer surface [6]. In order to solve this issue, carbon materials [7], metals [8] and more recently graphite/graphene [9,10] were employed as conductive additives. Indeed, these fillers may be added to the polymer matrix by different methods to confer electrical conductivity properties as long as their concentration is high enough to produce conduction pathways [11]. Unfortunately, the formation of a conducting percolated network is strictly related to the filler optimal dispersion within the polymer matrix, which is typically challenging. To enhance particles dispersion, a chemical modification may be exploited to improve compatibility with the polymer [12]. However, this implies laborious and not always environmental friendly processes.

It is also worth noting that, despite the use of PLA in packaging has emerged as a sustainable alternative to traditional polymers, no specific studies dealing with the modification of PLA to match antistatic application were reported in literature.

The third key property for packaging materials is transparency, which is usually affected by the additives and particles added to the pristine polymer to enhance gas barrier and/or surface electrical conductivity.

It is thus apparent that the development of biopolymer films suitable to be used in the antistatic packaging field should take into account several issues. Firstly, in order to maintain the sustainable features of the polymer, it is mandatory to apply low cost and sustainable methods involving, for instance, the modification of the polymer surface. The designed approach should then produce films characterized by high transparency, low gas permeability and good antistatic properties. From this point of view, the use of the Layer-by-Layer (LbL) technique represents an ideal solution due to its coating design freedom, green features and the possibility to use carbon-based material as layer components [13]. As far as PLA is concerned, the LbL was mainly applied in the biomedical field [14,15]. To the best of the authors' knowledge this manuscript represents the first attempt employing the LbL in order to produce antistatic PLA.

Graphite oxide (GO) has been recently employed as carbon-based material in LbL assemblies [16]. GO is negatively charged in aqueous solution because of its functional groups such as carboxylic acid and phenolic hydroxyl groups [17]. Positively charged polyelectrolytes were selected as counterparts for the LbL assembly. Chemical reduction and annealing post treatments were employed in order to recovery the electrical properties of the LbL assembled multilayered GO films [18]. It was found that, in reduced GO LbL films, both the sheet resistance and the optical transmittance can be effectively controlled by changing the number of bi-layers.

In the present work, focusing on the development of poly(L-lactide) (PLLA) films applicable in the field of antistatic packing, we applied the LbL process as an environmental friendly method capable of maintaining the bulk properties of the biopolymer while modifying its surface. Here, positively charged chitosan (CH) or branched polyethylenimine (BPEI) have been coupled with graphite oxide (GO) (Fig. 1) in a LbL fashion. In order to maintain the procedure as sustainable as possible the deposition process was performed in water and the subsequent GO reduction was accomplished by water-soluble reducing agent. The characteristics of the modified films, in terms of morphology, wettability, permeability and surface electrical conductivity, were studied as function of the number of deposited bi-layers and the type of positive polyelectrolyte.

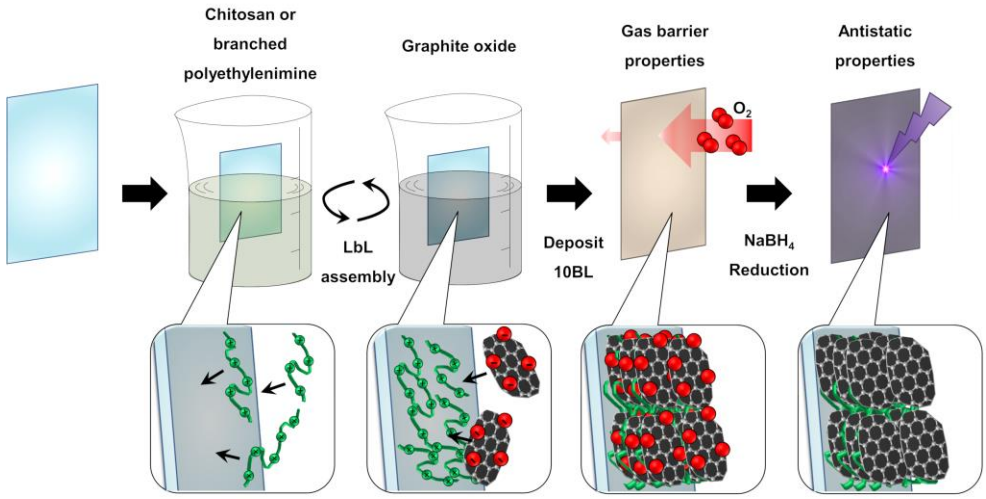

Fig. 1. Scheme of the Layer-by-layer deposition procedure.

2. Materials and methods

2.1. Materials

Poly (L-lactide) (PLLA) is a commercial product purchased from Nature Works Co. Ltd. U.S.A. (2002D, M_n = 100.000 g/mol) with a residual monomer content less than 0.3 % by mass. Dicloromethane, sodium borohydride ($NaBH_4$), branched poly(ethylene imine) (BPEI, M_w ~25.000 g/mol) and chitosan (CH, M_w ~190.000-310.000 g/mol) were purchased from Sigma-Aldrich. Graphite oxide (GO), as 1 wt.-% suspension in water, was purchased from AVANZARE Innovacion Tecnologica (Navarrete-La Rioja, Spain). Solutions and suspensions employed were prepared using ultrapure water having a resistance of 18.2 MΩ, supplied by a Q20 Millipore system (Milano, Italy). Single side polished (100) silicon wafer was used to study the growth of the layers. BPEI solution had a solid content of 1 wt.-% and chitosan 0.5 wt.-%; the pH was kept unmodified for BPEI while it was adjusted to 4 with 0.25 wt.-% of acetic acid for chitosan.

2.2. PLLA film preparation and Layer-by-Layer (LbL) deposition on films

Films were obtained by solubilizing PLLA pellets at a final concentration of 0.5 wt.-% in dicloromethane. This solution (10 mL) was then casted in a Petri dish (10 cm diameter) and dried in air. Then, the solidified films were further dried in vacuum for 4 hours at 40 °C and 4 hours at 80 °C. Finally, the films were cut into squares of size 3.5 × 3.5 cm^2 to be used for the LbL deposition.

PLLA films were alternately immersed into negatively and positively charged suspensions. The first immersion period for the BPEI activation layer was set at 20 min, in order to promote the homogeneous growth of the subsequent BPEI/GO bi-layer (BL). These layers were obtained with 4 min of dipping. After each immersion step, the film was washed with deionized water for 1 min to remove the excess of ionic species and dried by a flow of compressed air. The process was repeated until films characterized by a different number of BL (5, 10 and 15) were prepared. The same procedure was applied for the LbL deposition based on CH. The samples are coded by the type and the number of BL (as an example: PLLA_BPEI_GO_15 indicates 15 BL of BPEI and GO onto PLLA).

$NaBH_4$ solution in water with a concentration of 0.1 mol/L was used for the reduction of GO-based films (GOr in the code of the films). The films were dip in 20 mL of the above solution for two hours at room temperature, then they were extensively washed and finally dried in vacuum overnight at 40 °C.

Si wafers employed to monitor the coating growth were alternately dipped into solutions of positively charged polyelectrolytes (BPEI or CH) and negatively charged (GO) in order to deposit a coating consisting of 10 BL repetitive unit. The deposition times were set as described for PLLA. After each adsorption step, the substrate was washed by static dipping in deionized water and then dried by a flow of compressed air.

2.3. Characterization

Fourier Transform InfraRed (FT-IR) spectroscopy was used to monitor the growth of the LbL assembly using a Perkin Elmer Frontier FT-IR/FIR spectrophotometer (16 scans and 4 cm^{-1} resolution). IR spectra were acquired after each deposition step.

A Zeiss Supra 40 VP field emission scanning electron microscope (FE-SEM) equipped with a backscattered electron detector was used to examine the composite morphologies. The samples were sputter-coated with a thin carbon layer using a Polaron E5100 sputter coater.

Contact angle measurements were carried out by a Basler as A780 contact angle analyzer, using the sessile drop method, and the Oneattension software at a minimum of 2 different locations for each film.

Oxygen and water vapor permeability measurements were performed using an Extraperm apparatus (Extra Solutions, Italy). The test were performed at 23°C in dry (0% R.H.) and humid (50% R.H) conditions for oxygen permeability while water vapor permeability was assessed at 23°C and 50% R.H. Due to the small size of the prepared films, the samples were tested using an aluminum mask to reduce the exposed area to 2.01 cm^2.

Conductivity tests, which were performed accordingly with the ASTM D257 method, were carried by applying a picommater (Keithley) and by using films of 1×1 cm (with a thickness of ca. 100 μm). The instrument was zeroed before the 300 V voltage application. Two rectangles of silver glue (3×8 mm), spaced 3 mm apart, were deposited on the films in order to form the electrical contact. The surface resistivity (ρ_s) was calculated by applying the following equation:

$\rho_s = R_s P/G$ where R_s is the surface resistance, P is the perimeter of electrodes and G is the gap between electrodes.

3. Results and discussion

In this work, the surface modification of poly(L-lactide) (PLLA) films was performed by applying the Layer by Layer (LbL) technique and by using two types of positively charged polyelectrolytes, chitosan (CH) and branched polyethylenimine (BPEI). Indeed, these molecules, holding amino groups and being positively charged, are potentially capable of interacting with the surface of PLLA as well as of promoting the GO deposition. The concentrations of CH and BPEI were chosen on the basis of the conditions reported in the literature and on their solubility [19,20].

The coating growth was monitored by IR spectroscopy. The spectra of neat CH, neat BPEI and GO are reported in Fig. 1S. CH (Fig. 1Sa) shows peaks at approximately 3380 and 3296 cm^{-1} associated to O−H and N−H stretching, while signals at 2922, 2868, 1406 and 1320 cm^{-1} were assigned to C-H bond [19]. The sharp peak at 1578 and the shoulder at 1636 cm^{-1} can be attributed to asymmetric and symmetric stretching vibration mode of the protonated amine NH_3^+. The latter signal is also ascribed to O-H stretching vibration in residual water. The peaks at 1070 and 1140 cm^{-1} were assigned to pyranose rings and amino groups. BPEI shows a similar spectrum (Fig. 1Sb) with bands at 3320 (N-H stretching), 2947, 2832, 1466 and 1299 cm^{-1} (C-H bond), 1555 cm^{-1} (N-H bending), 1405 and 1031 cm^{-1} (C-N stretching) [20]. Neat GO (Fig. 1Sc) shows a broad band at 3346 cm^{-1} which can be assigned to the stretching mode of O-H group. The main signals are related to COOH functional groups and are found at 1616 and 1410 cm^{-1} for the deprotonated form COO^- (asymmetric and symmetric stretching, respectively) and 1704 cm^{-1} for C=O in the undissociated form. The peaks at 1194 and 1038 cm^{-1} may be attributed to C-OH and C-O, respectively [21].

The LbL assemblies of the CH/GO and BPEI/GO systems on model silicon substrate are reported as 3D plot in Fig. 2, along with the evolution in absorbance for selected functional groups as a function of deposited BL number and the cross sections of 10 BL coatings.

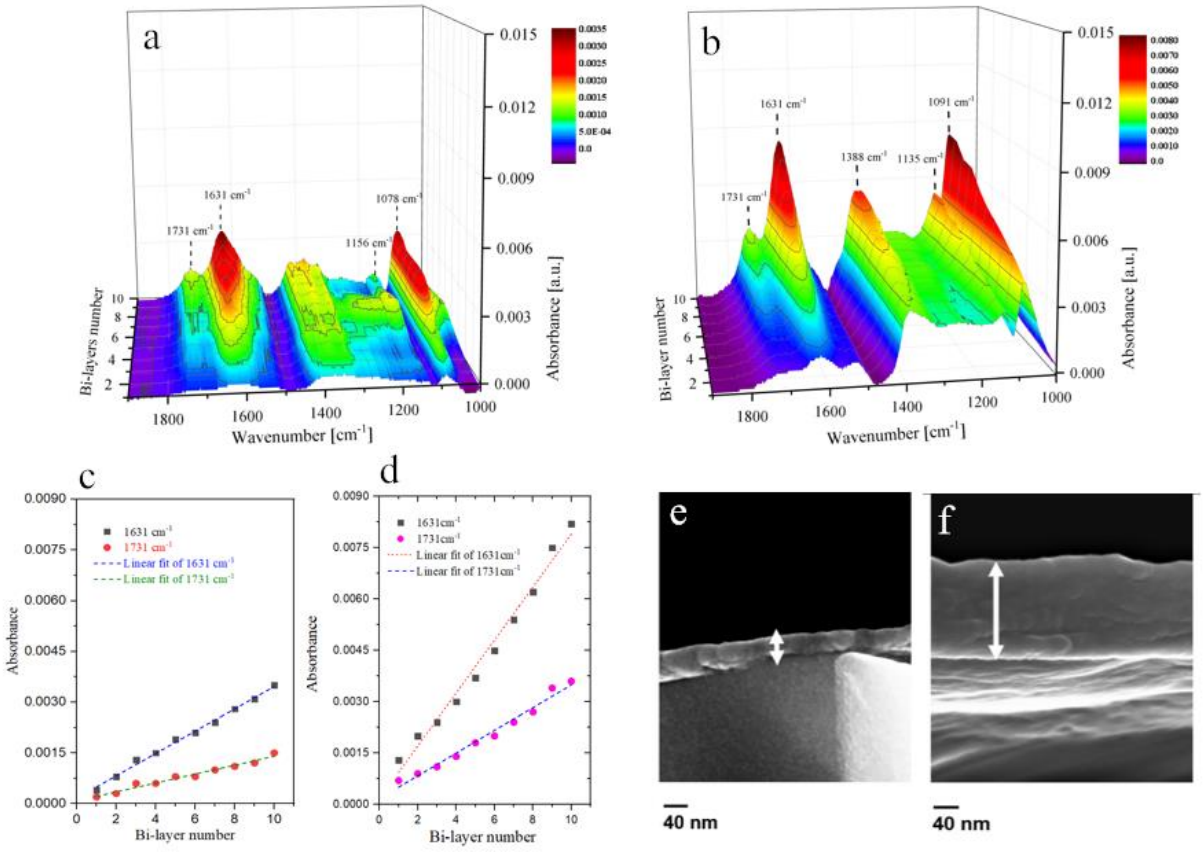

Fig. 2. Coating growth as a function of each deposited BL by infrared spectroscopy of restricted IR region between 1000 and 2000 cm^{-1} of: (a) CH/GO and (b) BPEI/GO on model silicon surface. Evolution of the signals at 1631 and 1731 cm^{-1} as function of bi-layer number of: (c) CH/GO and (d) BPEI/GO. SEM micrographs of the cross section performed on 10 BL deposited on silicon wafer of: (e) of CH/GO and (f) BPEI/GO.

As far as CH/GO is concerned, the characteristic signals of both components can be found at 1115, 1185, 1288, 1495 and 1701 cm^{-1}. In particular, the signals at 1631 and 1731 cm^{-1} (related

to GO) turned out to grow proportionally to the number of deposited BL (Fig. 2c), thus confirming the occurrence of a LbL assembly, in agreement with what previously reported in the literature [22] . In the case of the films based on BPEI (Fig. 2b), the observed signals appear more intense with respect to CH/GO. In particular, the characteristic peaks associated to dissociated carboxylic groups on GO are well visible at 1631 and 1388 cm^{-1} (asymmetric and symmetric stretching, respectively). These signals appear more intense with respect to those found in neat GO and CH/GO assembly. This is explained by considering that the ionization degree of GO carboxyl groups is pH dependent. Indeed, while for neat GO and CH/GO IR spectra are collected after adsorption from acidic pH, during BPEI adsorption the adsorbed GO is exposed to basic pH values (pH = 9-10) that promote the dissociation of carboxyl groups [23,24]. In the final LbL assembly, this phenomenon results in a strong increase of the signals associated to COO^- and a decrease of the COOH peak. In addition, the signals related to COO^- show a shift with respect to neat GO; this is ascribed to the interaction of the functional group with the BPEI protonated amines and further highlights the occurrence of a LbL deposition through electrostatic interactions. As observed for the CH-based system, the peaks characteristic of GO linearly increased as function of BL number (Fig. 2d). The remarkable difference in intensity at 10 BL between the two systems suggests that BPEI/GO grows thicker than CH/GO. This is further confirmed by FE-SEM observations performed on the cross-section of 10 BL assemblies (Fig. 2e and 2f) where thicknesses of 40 and 200 nm were evaluated for CH- and BPEI-based systems, respectively. This can be ascribed to the different nature of the employed polycations. Indeed, during BPEI adsorption the increased dissociation of GO carboxyl groups in the previously adsorbed layer results in an increased negative charge to be compensated. Similarly, the acidic pH of GO suspension improves the protonation degree of BPEI and results in more GO

adsorbed. Such phenomena do not occur in the CH-based assembly due to the acidic pH of the chitosan solution.

The influence of the treatment on the film wettability was studied by static contact angle measurements on neat PLLA and films treated by a different number of deposition BL (from 5 to 15) (Fig. 3). The values obtained are summarized in Table 1. The neat PLLA film (Fig. 3a and 3e) was found to hold a contact angle of ca. 80°, in agreement with the data reported in the literature [25]. The deposition of a single layer of BPEI or CH did not produce a significant modification of the material wettability and the measured contact angles (85° for CH based film and 78° for BPEI based film) were in agreement with previous reports for the two neat polymers [26,27]. On the contrary, the deposition of an assembly containing GO resulted in a reduction of the wettability, which value turned out to decrease by increasing the number of the deposition BL. This was more relevant for BPEI-based assemblies. Indeed, in the case of CH, the maximum contact angle after15 BL was 54.8° while for PLLA_BPEI_GO_15 reached 30.2°.

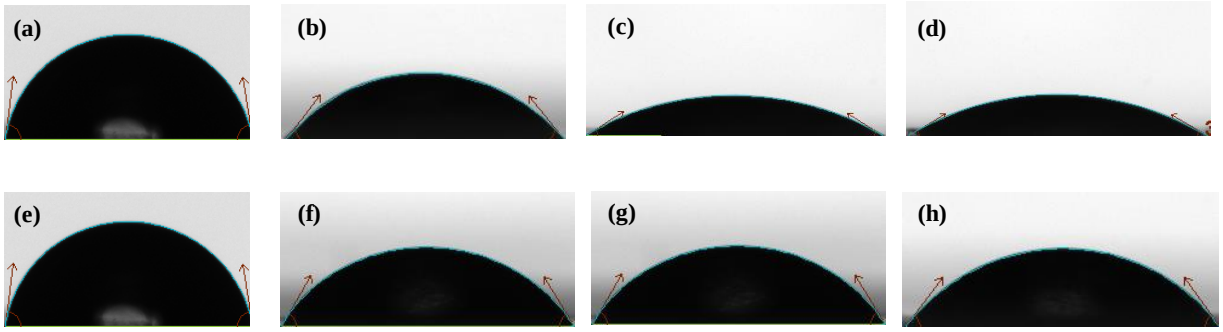

Fig. 3. Water contact angle images of: (a) PLLA, (b) PLLA_BPEI_GO_5, (c) PLLA_BPEI_GO_10, (d) PLLA_BPEI_GO_15, (e) PLLA, (f) PLLA_CH_GO_5, (g) PLLA_CH_GO_10 and (h) PLLA_CH_GO_15.

Table 1. Contact angle of the neat PLLA film and of the LbL treated films.

Sample code	Contact angle (°)	Sample code	Contact angle (°)
PLLA	80.6 ± 0.2	PLLA	80.6 ± 0.2
PLLA_BPEI_GO_5	50.5 ± 0.3	PLLA_CH_GO_5	59.6 ± 0.3
PLLA_BPEI_GO_10	31.7 ± 0.5	PLLA_CH_GO_10	59.6 ± 0.1
PLLA_BPEI_GOr_10	68.3 ± 0.5	PLLA_CH_GOr_10	77.0 ± 0.3
PLLA_BPEI_GO_15	30.2 ± 0.5	PLLA_CH_GO_15	54.8 ± 0.1

Wettability data for systems containing GO, either on the surface or in the bulk, are reported in the literature [28-32]. In the case of bulk addition of GO within a polymer, the wettability turned out to depend on the matrix characteristics, the GO concentration and its functionalization [28]. The presence of GO typically resulted in hydrophilic surfaces, with water contact angles smaller than or equal to 45° [29-32]. Nevertheless, different aspects have to be taken into account. Indeed, when GO is deposited on a surface, as in the case of our systems, the substrate effect as well as the homogeneity of the deposition might influence the surface wettability. Moreover, as previously mentioned, the characteristics of graphene oxide, in terms of its functionalization degree, was found to affect the contact angle values. On the basis of these aspects, it is possible to hypothesize that by increasing the number of the deposition layers, the homogeneity of the deposited coatings increases. Indeed, as reported in Table 1, the variation of the contact angles turned out to decrease by increasing the number of deposition BL and reached a plateau after 10 BL. The different values between CH and BPEI-based systems can be ascribed to the different

contributions of the employed polycations and the different percentage of ionized groups/ionic bonds in the final assembly as evaluated by IR spectroscopy.

On this basis, considering the slight difference between 10 and 15 BL, only 10 BL coatings were further investigated. This choice was mainly related to the need to keep the developed approach as simple as possible in order to make it more easily applicable. In this light, it is desirable to use as few depositions as possible.

Moreover, also the different wettability obtained by using the two types of polycations might be explained by taking into account the morphology of the deposition, which should depend on the specific interactions of the molecules with the polymer surface and with GO.

In order to assess the film morphology, both optical microscopy and FE-SEM measurements were carried out. The photos of the neat and the 10 BL treated films, are reported in Fig. 2S. The above images evidenced for the formation of a homogeneous coating at micron scale, highlighting the presence of GO nanoplatelets of variable dimensions. FE-SEM micrographs of 10 BL samples (Fig. 4) evidenced a wrinkled morphology typical of GO-based coatings while showing further differences in the two film surface morphologies. Indeed, while the film based on BPEI (Fig. 4a) was characterized by a rather flat and a homogenous GO layer, the one prepared by using chitosan (Fig. 4b), displayed a much higher roughness.

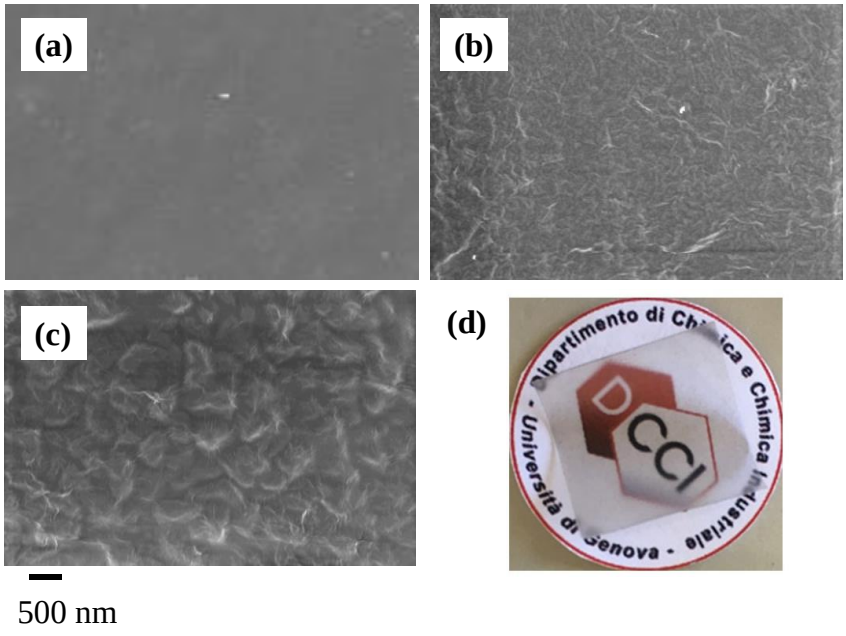

Fig. 4. SEM micrographs of: (a) PLAA, (b) PLLA_BPEI_GO_10 and (c) PLLA_CH_GO_10. (d) Photograph of PLLA_BPEI_GO_10 film after reduction.

As previously mentioned, one key feature for the films applicability is related to their transparency. Digital images of the films after the reducing treatment highlight the characteristic black color typical of graphite while also showing a good transparency of the LbL treated film (Fig. 4d). This demonstrates that, conversely to bulk modification, this LbL treatment allows to maintain a fairly good transparency of the coated film.

With the aim at obtaining films characterized by surface electrical conductivity, the GO deposited on the surface of the PLLA films was reduced by sodium borohydride ($NaBH_4$) [33]. As reported in the literature, contact angle measurements can give evidence of the reducing

occurrence by showing a decreased wettability [33]. For example, in the case of GO nanopaper, the contact angle increased from 45.1° to 67.3° after aluminum reduction at 100-200 °C [27]. Similarly, Some et al. [34] described a reduction treatment under light exposure based on sodium benzophenone or sodium benzophenone in the presence of hydrazine, which increased the contact angle of GO films from 48.3° to 98.9°. As far as samples prepared in this work are concerned, values reported in Table 1 and images in Fig. 3S clearly show an increase in contact angle for 10 BL films after reduction. This was more apparent for BPEI/GO system that displayed an overall increase of 38.1° with respect to the 17.7° increase measured for CH/GO. By comparing these values with those reported in the literature, it is possible to infer that the applied reduction treatment, although based on mild conditions, lead to a relevant increase of the surface hydrophobicity thus indicating a significant degree of reduction. The reduction of GO was also evaluated by means of IR spectroscopy (Fig. 4S). Only the BPEI/GO sample was evaluated as in the case of CH the presence of the oxygen contained in the polymer chemical structure might affect the results of the measurements. By comparing the spectra before and after reduction, it is possible to observe a decrement of the absorption bands at 1700 cm^{-1} and at 1100 cm^{-1}, which can be related to the oxygen-based groups. This further confirms the occurrence of a reduction reaction.

The barrier and permeability performances of PLA films have been widely studied because of the relevant impact of these features on the material applications [35,36]. Oxygen barrier properties in dry and humid conditions as well as water vapor permeability have been evaluated for neat PLLA and 10 BL treated films (Fig. 5 and Table 1S).

A common approach to improve PLA gas barrier properties is represented by the bulk inclusion of layered silicates that normally results in a 50% reduction in oxygen permeability but also

shows negative impact on the optical properties [35,36]. A more efficient approach is based on the LbL deposition of clay, which was found to decrease the oxygen permeability by 96% [37]. In this work, the films treated with BPEI/GO showed a 70 % reduction of the oxygen permeability both at low and at high relative humidity (RH). Such results can be ascribed to the well-known LbL brick and mortar structures where nanoplatelets are oriented parallel to the film surface and perpendicular to the gas flux. This creates a tortuous path towards the molecules of the permeating gas thus resulting in improved barrier performances. The performed reduction treatment leads to an increase of the permeability, which increment resulted to be slight at low RH and relevant only at high RH. On the other hand, CH/GO films showed a more limited decrease of the permeability. This finding is in agreement with the previous characterization that provided evidence of the formation of a thinner and rougher deposition layer for the chitosan-based films. Comparing the obtained results with the findings reported in the literature for LbL treated PLA, it is worth underlining that relevant variations in permeability were achieved only after 30-70 deposited BL [37-40]. On this basis, the results obtained by applying 10 BL of BPEI/GO system developed in this paper are similar to other 10 BL LbL systems comprising montmorillonite clay nanoplatelets or better than BPEI/nanocellulose coatings. Clearly, it is apparent that it is necessary to find a compromise between the number of deposited BL and the final material properties as a function of the selected application.

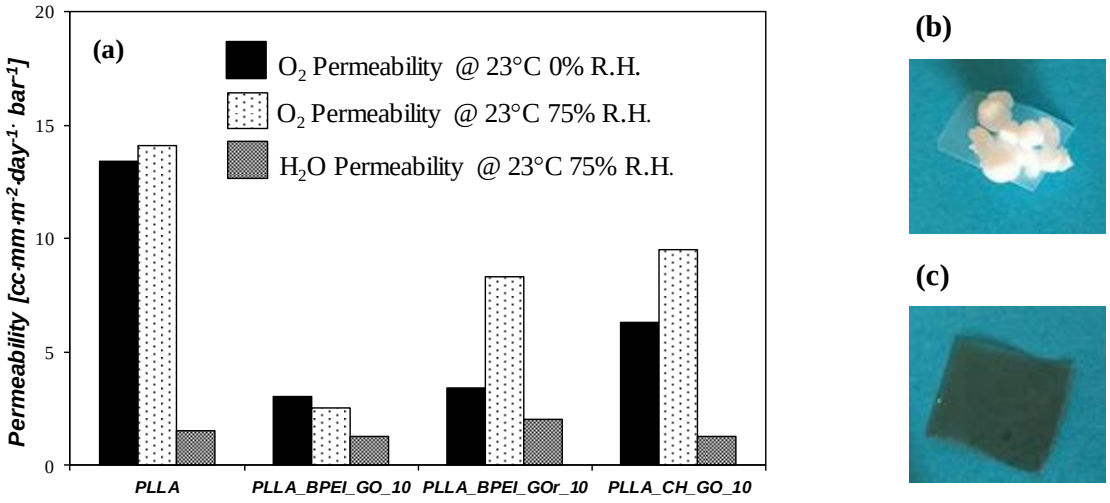

Fig. 5. (a) O_2 and H_2O permeability of: PLLA, PLLA_BPEI_GO_10, PLLA_BPEI_GOr_10 and PLLA_CH_GO_10, photos of: (b) PLLA and (c) PLLA_BPEI_GOr_10 films after rubbing them with a woolen cloth and putting in contact with polystyrene particles.

The effect of the surface treatment on the antistatic properties of the films was evaluated measuring the surface resistivity of the optimal formulation based on BPEI and employing a practical method to evaluate the achieved. Considering the Fig. 5b and 5c and the videos 5S (video of neat PLLA film) and 6S (video of PLLA_BPEI_GOr_10 films), it is apparent that the neat PLLA film, after being charged, was capable of attracting the polystyrene particles, while the coated PLLA did not retain those. Although the above method is very simple, it gives a preliminary indication of the antistatic features of the treated films, it being widely used in industry. A quantification of the effect of the coating was evaluated by accomplished surface resistivity (ρ_s) measurements by using a picommater. Indeed, ~~This effect is accompanied by~~ a decrease of the film surface resistivity from $6.3 \cdot 10^{12}$ Ohms/square for PLLA film to $7.3 \cdot 10^{11}$ Ohms/square for PLLA_BPEI_GOr_10 was found. Although the above decrement is not as high

as those reported in the literature for other systems [40,41], it has been demonstrated to be enough to result in an antistatic surface. From an overall point of view, the achieved barrier and antistatic properties make the developed BPEI/GO assembly a promising and attractive alternative to the classical antistatic packaging systems for PLLA.

4. Conclusions

In this work, modified poly(L-lactide) (PLLA) films with good oxygen barrier, transparency and antistatic properties were developed. This set of properties makes the prepared materials applicable in the antistatic packaging field. Indeed, the proposed approach involves the Layer-by-Layer (LbL) deposition of functional coatings comprising either deposition of chitosan (CH) or branched polyethylenimine (BPEI)) in combination with graphite oxide (GO). The characterization results evidenced the more effectiveness of BPEI with respect to CH as positive counterpart in the LbL assemblies. Coating growth was investigated by IR spectroscopy coupled with microscopy observations showing that the BPEI/GO system is capable of growing thicker while producing more homogeneous coatings than CH/GO. This was further confirmed by static contact angle measurements. Film coated by 10 BL BPEI/GO showed a 70% reduction in oxygen permeability in both dry and humid conditions. The same coating was subjected to a reduction post treatment capable to confer antistatic properties to the coated film. The conditions applied in the LbL deposition, with a limited number of bi-layers, and the subsequent reduction of GO, carried out in water and at room temperature, result in a sustainable and easily scalable method for the modification of polymer surface properties. This is of particular interest in the

case of biopolymers, such as PLA, allowing to extend their applicability range towards novel and attractive application, by the engineering of surface properties and retaining the bulk properties.

Supporting Information

FT-IR spectra of CH, BPEI and GO. Optical images of the neat PLLA film, PLLA_CH_GO_10 and PLLA_BPEI_GO_10. Water contact angle images of PLLA_BPEI_GO_10, PLLA_BPEI_GOr_10, PLLA_CH_GO_10 and PLLA_CH_GOr_10. FT-IR spectra of10 BL of BPEI/GO deposited on silicon wafer before reduction and 10 BL of BPEI/GO deposited on silicon wafer after reduction. Table of the permeability results. Videos showing the ability to capture polystyrene particles of PLLA film and PLLA_BPEI_GOr_10 film after rubbing them with a woolen cloth.

Acknowledgement

The China Scholarship Council is gratefully acknowledged for funding of the Ph.D. grant for K.L.

References

[1] Handbook of Biopolymers and Biodegradable Plastics, S. Ebnesajjad Ed., 2013 Elsevier Inc.

[2] L.-T. Lima, R. Auras, M. Rubino, Processing technologies for poly(lactic acid), Prog. Polym. Sci. 33 (2008) 820–852.

[3] V. Nagarajan, A.K. Mohanty, M. Misra, Perspective on polylactic acid (PLA) based sustainable materials for durable applications: focus on toughness and heat resistance, ACS Sustainable Chem. Eng. 4 (2016) 2899−2916.

[4] A. Zheng, X. Xu, H. Xiao, N. Li, Y. Guan, S. Li, Antistatic modification of polypropylene by incorporating Tween/modified Tween, Appl. Surf. Sci. 258 (2012) 8861–8866.

[5] A. Tsurumaki, S. Tajim, T. Iwata, B. Scrosati, H. Ohno, Evaluation of ionic liquids as novel antistatic agents for polymethacrylates, Electrochim. Acta 248 (2017) 556–561.

[6] J.C. Costa, M. Oliveira, A.V. Machado, S. Lanceros-Méndez, G. Botelho, Effect of antistatic additives on mechanical and electrical properties of polyethylene foams, J. Appl. Polym. Sci. 112 (2009) 1595–1600.

[7] M. Zhang, C. Zhang, Z. Du, H. Li, W. Zou, Preparation of antistatic polystyrene superfine powder with polystyrene modified carbon nanotubes as antistatic agent, Compos. Sci. Technol. 138 (2017) 1-7.

[8] H. Jiang, K.S. Moon, Y. Li, C.P. Wong, Surface functionalized silver nanoparticles for ultrahigh conductive polymer composites, Chem. Mat. 18 (2006) 2969–2973.

[9] Q. Wang, Y. Wang, Q. Meng, T. Wang, W. Guo, G. Wub, L. You, Preparation of high antistatic HDPE/polyaniline encapsulated graphene nanoplatelet composites by solution blending, RSC Adv. 7(2017) 2796–2803.

[10] H. Wang, G. Xie, M. Fang, Z. Ying, Y. Tong, Y. Zeng, Electrical and mechanical properties of antistatic PVC films containing multi-layer graphene, Compos. Part B 79 (2015) 444-450.

[11] R. Sengupta, M. Bhattacharya, S. Bandyopadhyay, A.K. Bhowmick, A review on the mechanical and electrical properties of graphite and modified graphite reinforced polymer, Progr. Polym. Sci. 36 (2011) 638-670.

[12] M. Pöllänen, S. Pirinen, M. Suvanto, T.T. Pakkanen, Influence of carbon nanotube–polymeric compatibilizer masterbatches on morphological, thermal, mechanical, and tribological properties of polyethylene, Compos. Sci. Techol. 71 (2011) 1353-1360.

[13] J.J. Richardson, J. Cui, M. Björnmalm, J.A. Braunger, H. Ejima, F. Caruso, Innovation in Layer-by-Layer assembly, Chem. Rev. 116 (2016) 14828-14867.

[14] A. El Fagui, V. Wintgens, C. Gaillet, P. Dubot, C. Amiel, Layer-by-Layer coated PLA nanoparticles with oppositely charged β-Cyclodextrin polymer for controlled delivery of lipophilic molecules, Macromol. Chem. Phys. 215 (2014) 555−565.

[15] R. Hashide, K. Yoshida, Y. Hasebe, S. Takahashi, K. Sato, J. Anzai, Insulin-containing layer-by-layer films deposited on poly(lactic acid) microbeads for pH-controlled release of insulin, Colloids Surf. B 89 (2012) 242–247.

[16] T. Lee, S.H. Min, M. Gu, Y.K. Jung, W. Lee, J.U. Lee, D.G. Seong, B.-S. Kim, Layer-by-Layer assembly for graphene-based multilayer nanocomposites: Synthesis and applications, Chem. Mater. 27 (2015) 3785−3796.

[17] J.-T. Chen, Y.-J. Fu, Q.-F. An, S.-C. Lo, S.-H. Huang, W.-S. Hung, C.-C. Hu, K.-R. Lee, J.-Y. Lai, Tuning nanostructure of graphene oxide/polyelectrolyte LbL assemblies by controlling pH of GO suspension to fabricate transparent and super gas barrier films, Nanoscale 5 (2013) 9081-9088.

[18] L.G. Guex, B. Sacchi, K.F. Peuvot, R.L. Andersson, A.M. Pourrahimi, V. Ström, S. Farris, R.T. Olsson, Experimental review: Chemical reduction of graphene oxide (GO) to reduced graphene oxide (rGO) by aqueous chemistry, Nanoscale 9 (2017) 9562–9571.

[19] D. Battegazzore, A. Frache, F. Carosio, Sustainable and high performing biocomposites with chitosan/sepiolite Layer-by-Layer nanoengineered interphases, ACS Sustainable Chem. Eng. 8 (2018) 9601-9605.

[20] Y. Li, X. Wang, J. Sun, Layer-by-layer assembly for rapid fabrication of thick polymeric films, Chem. Soc. Rev. 41 (2012) 5998–6009.

[21] S. Rodríguez-García, R. Santiago, D. López-Díaz, M.D. Merchán, M.M. Velázquez, J.L.G. Fierro, J. Palomar, Role of the structure of graphene oxide sheets on the CO_2 adsorption properties of nanocomposites based on graphene oxide and polyaniline or Fe_3O_4-nanoparticles, ACS Sustainable Chem. Eng. 7 (2019) 12464−12473.

[22] L. Maddalena, F. Carosio, J. Gomez, G. Saracco A. Fina, Layer-by-layer assembly of efficient flame retardant coatings based on high aspect ratio graphene oxide and chitosan capable of preventing ignition of PU foam, Polym. Degrad. Stabil. 152 (2018) 1-9.

[23] D. Battegazzore, J. Alongi, A. Frache, L. Wågberg, F. Carosio, Layer by Layer-functionalized rice husk particles: A novel and sustainable solution for particleboard production, Mater. Today Comm. 13 (2017) 92-101.

[24] E. Kharlampieva, S.A. Sukhishvili, Ionization and pH stability of multilayers formed by self-assembly of weak polyelectrolytes, Langmuir 19 (2003) 1235-1243.

[25] L. Gardella, S. Colonna, A. Fina, O. Monticelli, A novel electrostimulated drug delivery system based on PLLA composites exploiting the multiple functions of graphite nanoplatelets, ACS Appl. Mater. Interfaces 8 (2016) 24909−24917.

[26] Y. Luo, X. Pan, Y. Ling, X. Wang, R. Su, Facile fabrication of chitosan active film with xylan via direct immersion, Cellulose 21 (2014) 1873–1883.

[27] P. Sengupta, B.L.V. Prasad, Surface modification of polymers for tissue engineering applications: arginine acts as a sticky protein equivalent for viable cell accommodation, ACS Omega 3 (2018) 4242-4251.

[28] W.K. Chee, H.N. Lim, N.M. Huang, I. Harrison, Nanocomposites of graphene/polymers: a review, RSC Adv. 5 (2015) 68014-68051.

[29] D. Wan, C. Yang, T. Lin, Y. Tang, M. Zhou, Y. Zhong, F. Huang, J. Lin, Low-temperature aluminum reduction of graphene oxide, electrical properties, surface wettability, and energy storage applications, ACS Nano 6 (2012) 9068–9078.

[30] W. Yi, H. Wu, H. Wang, Q. Du, Interconnectivity of macroporous hydrogels prepared via graphene oxide-stabilized pickering high internal phase emulsions, Langmuir 32 (2016) 982−990.

[31] Z. Zheng, X. Zheng, H. Wang, Q. Du, Macroporous graphene oxide-polymer composite prepared through pickering high internal phase emulsions, ACS Appl. Mater. Interfaces 5 (2013) 7974−7982.

[32] S.C. Hernández, C.J.C. Bennett, C.E. Junkermeier, S.D. Tsoi, F.J. Bezares, R. Stine, J.T. Robinson, E.H. Lock, D.R. Boris, B.D. Pate, J.D. Caldwell, T.L. Reinecke, P.E. Sheehan, S.G. Walton, Chemical gradients on graphene to drive droplet motion, ACS Nano 7 (2013) 4746–4755.

[33] L.G. Guex, B. Sacchi, K.F. Peuvot, R.L. Andersson, A.M. Pourrahimi, V. Ström, S. Farris, R.T. Olsson, Experimental review: Chemical reduction of graphene oxide (GO) to reduced graphene oxide (rGO) by aqueous chemistry, Nanoscale 9 (2017) 9562–9571.

[34] S. Some, S. Kim, K. Samanta, Y. Kim, Y. Yoon, Y. Park, S.M. Lee, K. Lee, H. Lee, Fast synthesis of high-quality reduced graphene oxide at room temperature under light exposure, Nanoscale 6 (2014) 11322–11327.

[35] N. Najafi, M.C. Heuzey, P.J. Carreau, Polylactide (PLA)-clay nanocomposites prepared by melt compounding in the presence of a chain extender, Compos Sci Technol. 72 (2012) 608–615.

[36] Y. Guo, K. Yang, X. Zuo, Y. Xue, C. Marmorat, Y. Liu, C.-C. Chang, M.H. Rafailovich, Effects of clay platelets and natural nanotubes on mechanical properties and gas permeability of poly (lactic acid) nanocomposites, Polymer 83 (2016) 246- 259.

[37] A.J. Svagan, A. Åkesson, M. Cárdenas, S. Bulut, J.C. Knudsen, J. Risbo, D. Plackett, Transparent films based on PLA and montmorillonite with tunable oxygen barrier properties, Biomacromolecules 13 (2012) 397−405.

[38] G. Laufer, C. Kirkland, A.A. Cain, J.C. Grunlan, Clay–chitosan nanobrick walls: Completely renewable gas barrier and flame-retardant nanocoatings, ACS Appl. Mater. Interfaces 4 (2012) 1643-1649.

[39] C. Aulin, E. Karabulut, A. Tran, L. Wågberg, T. Lindström, Transparent nanocellulosic multilayer thin films on polylactic acid with tunable gas barrier properties, ACS Appl. Mater. Interfaces 5 (2013) 7352-7359.

[40] Q. Wang, Y. Wang, Q. Meng, T. Wang, W. Guo, G. Wub, L. Youa, Preparation of high antistatic HDPE/polyaniline encapsulated graphene nanoplatelet composites by solution blending, RSC Adv. 7 (2017) 2796–2803.

[41] H. Wang, G. Xie, M. Fang, Z. Ying, Y. Tong, Y. Zeng, Electrical and mechanical properties of antistatic PVC films containing multi-layer graphene, Compos. B Eng. 79 (2015) 444-450.